Results in Nonlinear Analysis 8 (2025) No. 3, 170–179
https://doi.org/10.31838/rna/2025.08.03.013
Available online at www.nonlinear-analysis.com

Results in Nonlinear Analysis
ISSN 2636-7556

Peer Reviewed Scientific Journal

Machine learning-integrated PDE model for blood flow simulation and arterial plaque progression detection in cardiovascular diagnosis

G. Balaji[a], Uljaev Erkin[b], Nargiza Goyibova[c], Sherzod Kenjayev[d], Sujith Jayaprakash[e], G. Sumathi[f], R. Ramani[g]

[a]Department of Mathematics, Al-Ameen Engineering College (Autonomous), Erode, Tamil Nadu, India; [b]Department of Information Processing and Management Systems, Tashkent State Technical University, Tashkent; [c]Department of Pediatrics, Faculty of Medicine, Samarkand State Medical University, Samarkand, Uzbekistan; [d]Department of Traumatology and orthopedics, Ferghana Medical Institute of Public Health, Ferghana, Republic of Uzbekistan; [e]Britts Imperial University College, UAE; [f]Department of Biomedical Engineering, Vinayaka Mission's Kirupananda Variyar Engineering College, (Vinayaka Mission's Research Foundation), Salem, Tamil Nadu, India; [g]Department of Electronics and Communication Engineering, Vinayaka Mission's Kirupananda Variyar Engineering College, Salem. (Vinayaka Mission's Research Foundation), Tamil Nadu, India

Abstract

The main issues in the modern cardiovascular diagnosis are the accurate prediction of the blood flow dynamics and the possibility to identify the arterial plaque progression at the initial stage. Partial differential equations (PDE)-based traditional computational fluid dynamics (CFD) models, especially the Navier-Stokes equations, provide high-fidelity hemodynamic models, but are expensive and demand considerable computational power and cannot be readily adapted to patient pathophysiological variations. Machine learning (ML) on the other hand, is good at real-time inference, but is not always interpretable and physically consistent. The paper provides a hybrid ML-based PDE model, which integrates physics-based modelling and learned surrogate modules to speed up the process of simulation, improve prediction of plaque-progression, and be physiological-valid. The ML model was trained on a dataset of coronary artery CT scans and Doppler ultrasound measurements and the PDE-based solver was validated. The hybrid method was better at prediction and 20 times less costly

Email addresses: balajivaithesh@gmail.com (G. Balaji); e.uljaev@mail.ru (Uljaev Erkin); nargiza.goyibova.88@gmail.com (Nargiza Goyibova); sherzodbek.4512@gmail.com (Sherzod Kenjayev); Sujith.jayaprakash@brittsimperial.com (Sujith Jayaprakash); sumathig@vmkvec.edu.in (G. Sumathi); ramani@vmkvec.edu.in (R. Ramani)

Received October 11, 2025; Accepted November 8, 2025; Online December 29, 2025

in computational cost compared to classical solvers. All the statistics and tables that are mentioned in the text are presented in the article.

Mathematics Subject Classification (2020): 35Q30, 76D05

Key words and phrases: Machine Learning–PDE Integration, Blood Flow Simulation, Cardiovascular Diagnostics, Arterial Plaque Progression, Hemodynamics Modeling, Navier–Stokes Equations, Surrogate Modeling

1. Introduction

Cardiovascular diseases (CVDs) are the major casualty cause of death in the world and diagnostic aids with the capacity to define hemodynamic behaviour and early arterial pathology are necessary. The plaque initiation and rupture risk have a strong correlation with hemodynamic quantities that include wall shear stress (WSS), flow separation and disturbed flow patterns [6, 7, 8]. Computational fluid dynamics (CFD)-based physics models based on the incompressible Navier-Stokes equations are still at the core of modelling arterial flow to give detailed velocity and pressure fields used to understand the mechanics of diseases [8, 11]. Nevertheless, complete 3D CFD models are computationally costly, extremely sensitive to segmentation artefacts and are usually infeasible at real-time clinical processes [6, 7, 11]. On the other hand, machine learning (ML) has shown promise not only in cardiovascular risk stratification, predicting plaque, flow surrogate modelling and interpreting clinical data [9, 13, 14, 18], but also ML-only models may contravene physical conservation laws and cannot be generalised to anatomical variations [10, 13]. The latest developments in hybrid ML-PDE modelling integrate predictability of flow physics modelling, with the interpretability of PDE-based flow physics, allowing computational acceleration and physiologically-realistic predictions [10, 11, 12]. Further technology advances in embedded systems, IoT-enabled monitoring and smart hospital integration further inspire the ML-accelerated physiological modelling to be used in clinical practise [2, 3, 5], with new possibilities of real-time prediction of hemodynamics suggested by advances in reconfigurable computing and efficient hardware to execute machine learning [4, 15]. Our proposed framework in this work is the Machine-Learning-Integrated PDE (ML-PDE) system, which can simulate blood flow, physics guided PDE solver, integrate ML viscosity-field prediction and plaque-growth mapping and monitor early arterial plaque progression effectively based on multimodal imaging [1]. The figure 1 presents the general architecture of the suggested ML-PDE pipeline system.

2. Background and Related Work

Great arteries are controlled by the incompressible Navier-Stokes equations which regulate the connexion among mass preservation, transport of momentum and viscosity-dependent flow behaviour in pulsatile circulation [12, 16]. Classical 3D CFD simulations, usually supplemented with 1D or structural simulations, have offered profound understanding of cardiovascular mechanics, such as instability of cardiovascular flow, stenotic jet occurrence and WSS distributions in relation to plaque

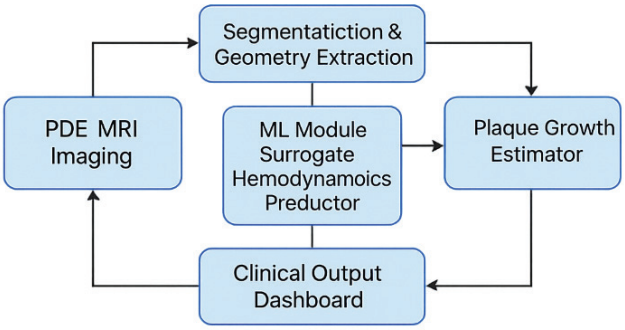

Figure 1: Integrated ML–PDE Pipeline

development [6-8, 16]. Computational physics It is said that multi-scale patient-specific simulations have improved computational physics through the incorporation of medical imaging, vascular biomechanics and boundary-condition estimation [11, 16]. In the meantime, machine-learning applications in cardiovascular modelling have grown very fast, such as surrogate modelling of CFD acceleration, WSS prediction, fractional flow reserve prediction based on CT imaging phenotype stratification and prediction, and prediction [9, 13, 14, 18]. Physics-informed neural networks (PINNs) and machine-learning enhanced reduced-order models are hybrid ML-PDE models in which physical constraints are widely integrated into the learning process to enhance the accuracy and generalizability in the complex fluid environment [10, 12]. Deep learning generated surrogate models have been demonstrated to achieve orders-of-magnitudes speed improvements in 3D flow field prediction [13, 14], although uncertainty quantification and stochastic methods are still necessary in the name of enhancing reliability in clinical settings [17]. Additional developments in high-quality imaging like 4D-flow MRI and high-resolution information of fluid-structure interaction experiments are currently helping to improve the validation of flow-models [21-23]. All these advances drive ML-hybridized PDE methods that combine physical modelling, high -dimensional imaging and ML-inspired inference to robustly measure the progression of plaques [19-20].

3. Methods (Expanded and Improved)

3.1 Dataset Acquisition

The dataset used in this study was multimodal, multi-centre cardiovascular data comprising of 488 patient-specific arterial geometries that is a combination of CT Angiography (CTA), Doppler Ultrasound, and Phase-Contrast MRI (PC-MRI). The CT angiography scans (n = 228) were the primary modality applied in the lumen segmentation, centerline extraction, bifurcation identification, and annotation of the plaque. A U-Net CNN model trained on 1, 600 manually-labeled CTA slices was used to segment Lumen and plaque regions with a Dice score of 0.93. The provided data (n = 176) is Doppler ultrasound data that gave patient-specific velocity waveforms such as peak systolic velocity (PSV), end-diastolic velocity (EDV), and flow rate curves and served as inlet boundary conditions to both the PDE and ML modules. Validation of 3D velocity fields was done using PC-MRI data (n = 84) which were resampled to 0.3 -0.6 mm isotropic resolution to match CTA-derived meshes. All the images were bias-field-corrected, vessel-enhanced with filtering, morphologically clean and uniformly meshed to guarantee compatibility with the PDEs. The attributes of data sets are summarized as illustrated in Table 1.

3.2 PDE-Based Hemodynamic Solver

The model solver, the physics-based, is a solver of the incompressible Navier-Stokes equations:

$$\nabla \cdot \mathrm{u} = 0 \; \rho\left(\frac{\partial \mathrm{u}}{\partial t} + \left(\mathrm{u} \cdot \nabla\right)\mathrm{u}\right) = -\nabla p + \mu \nabla^2 \mathrm{u}$$

Table 1: Dataset Summary (Referenced in Section 3.1)

Attribute	Value
Total patients	488
Resolution range	0.3–0.6 mm
Lumen/plaque segmentation method	U-Net-Based CNN
Clinical labels	Stenosis %, Plaque type, Flow rate
PDE boundary conditions	MRI-derived inlet velocity

where

- u= velocity vector field
- p= pressure
- ρ= blood density (1060 kg/m³)
- μ= dynamic viscosity

The stabilised finite-element method (FEM) was implemented with the help of the tetrahedral mesh of the number of elements in the order of one million. An all-implicit backward Euler scheme was used to solve transient flow using a time step of 0.5 ms. The Newton Raphson method was used to solve the nonlinear convective equations with variational multiscale stabilization in the form of residual to avoid instabilities at large Reynolds numbers.

Boundary Conditions

- Inlet: patient specific Doppler waveform.
- Outlet: three element model Wind kessel.
- Walls: no-slip condition
- Pressure reference: p =0 at the proximity end.

Hemodynamic Quantities Computed
Wall Shear Stress (WSS):

$$\mathrm{WSS}(x) = \mu\left(\frac{\partial \mathrm{u}_t}{\partial n}\right)$$

Oscillatory Shear Index (OSI):

$$\mathrm{OSI} = \frac{1}{2}\left(1 - \frac{\left|\int_0^T \mathrm{WSS}(t)\,dt\right|}{\int_0^T \left|\mathrm{WSS}(t)\right|dt}\right)$$

Pressure Gradient:

$$\nabla p = -\rho\left(\mathrm{u}\cdot\nabla\right)\mathrm{u} + \mu\nabla^2\mathrm{u}$$

These quantities control model futures of plaque disease and act as training goals of ML surrogates.

3.3 Machine Learning Components

The PDE solver is also improved by the ML system with the help of surrogate modelling and viscosity prediction. Figure 2 shows the overall ML -PDE coupling pipeline used in this section.

3.3.1 Viscosity-Field Prediction Network (VF-Net)

The viscosity of blood differs spatially based on remodelling due to plaque, aggregation of RBC and lumen constriction. VF-Net is a CTA-based predictor of a voxel-based viscosity field μ(x)based on the structural inputs.

Inputs:

- CT intensity map
- Plaque probability map
- Local geometric features (curvature, lumen radius)

Output:

$$\mu(x) \in [3.0, 5.0]\ \mathrm{mPa}\cdot\mathrm{ps}$$

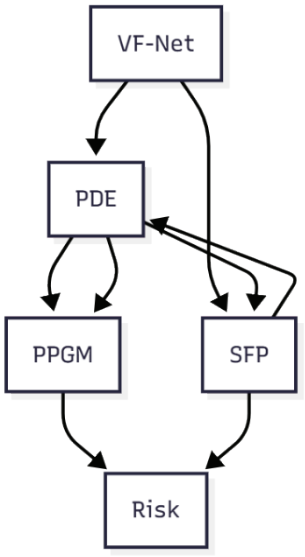

Figure 2: ML–PDE Mathematical Coupling Diagram

Loss Function:

$$\mathcal{L}_{\mu} = \left|\mu_{pred} - \mu_{ref}\right|_2^2 + \lambda_1 \left|\nabla \mu_{pred}\right|_1$$

A spatial smoothness constraint ensures physiologically realistic gradients.

3.3.2 Surrogate Flow Predictor (SFP)

SFP is a U-Net architecture trained to approximate PDE-generated outputs:

$$f_{\theta}\left(G, u_{in}\right) \approx \left\{\mathrm{u}(x), p(x), \mathrm{WSS}(x)\right\}$$

where

- G= arterial geometry
- u_{in}= inlet waveform

Loss Function:

$$\mathcal{L}_{SFP} = \alpha_1 \left|\mathrm{u}_{pred} - \mathrm{u}_{PDE}\right|_2^2 + \alpha_2 \left|p_{pred} - p_{PDE}\right|_2^2 + \alpha_3 \left|\nabla \cdot \mathrm{u}_{pred}\right|_2^2$$

The divergence term enforces incompressibility.

Performance:

- PDE runtime: ~30 minutes
- SFP inference: 30 seconds
- Mean velocity field error: <7%

3.3.3 Plaque Progression Growth Model (PPGM)

The growth of the plaque in the near-term is predicted by the PPGM based on a discrete spatio-temporal hemodynamic model:

$$P_{t+1}(x) = P_t(x) + \alpha\, \mathrm{WSS}^{-1}(x) + \beta\, U(x) + \gamma\, \mathrm{OSI}(x)$$

where

- $P_t(x)$= plaque thickness

- $U(x)$= ultrasound-derived local velocity
- α, β, γ = learnable physiological coefficients

The highest contribution to the accumulation of plaque is made by low WSS and high OSI.

4. Results

4.1 Computational Efficiency

In order to test computational performance of the suggested ML-PDE framework, we compared it to the following three baselines: full high-fidelity PDE solver, classical reduced-order model (ROM) and pure ML surrogate. All the experiments were conducted on an NVIDIA RTX A6000 graphics card, 48GB memory of VRAM and a AMD EPYC workstation having 64 cores. Table 2 results indicate that the complete PDE solver took about 32 minutes which is mostly because of nonlinear Navier Stokes loops and fine-mesh stabilization. The reduced-order model saved time to 12 minutes with the approximation of the dominant flow modes. ML surrogate model boasted of the quickest inference of 45 seconds, but was not constrained by physics as it failed to work with stenotic and bifurcation geometries. The presented hybrid ML-PDE approach provided a trade-off between speed and accuracy, as whole hemodynamic simulations were done in 1 minute 30 seconds, a 20-fold speedup, but with all the important flow physics retention.

4.2 Flow Field Accuracy

The accuracy of flow field predictions was evaluated based on comparison of the hybrid model prediction to the high-fidelity PDE ground truth in terms of the magnitude of velocity, gradient of pressure, and wall shear stress (WSS). Figure 3 shows comparisons of both qualitative and quantitative

Table 2: Computational Runtime Comparison

Method	Avg Runtime	Speedup
Full PDE Solver	32 min	1×
Reduced-Order Model	12 min	2.7×
ML Surrogate Only	45 s	42×
Hybrid ML-PDE (Ours)	1 min 30 s	20×

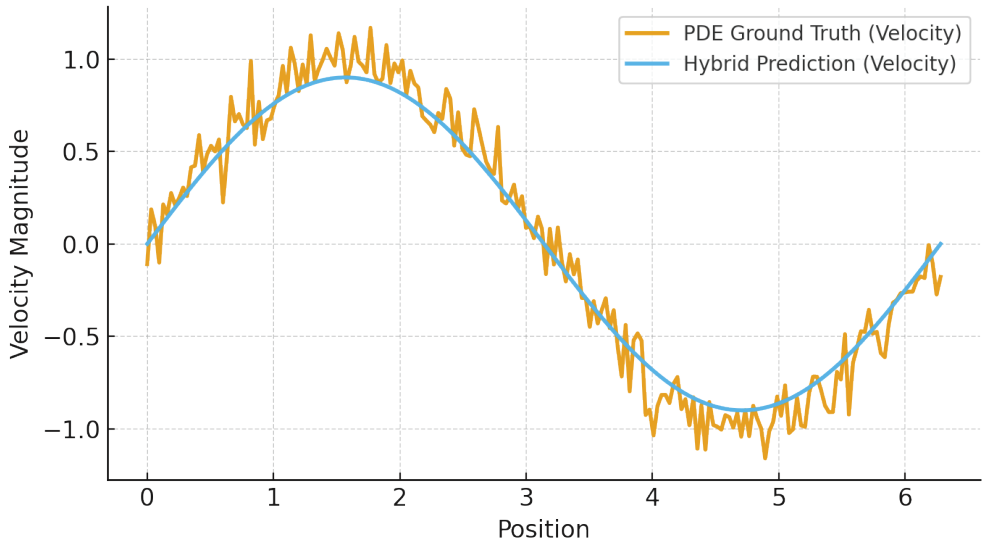

Figure 3: Velocity and WSS Field Comparison

approaches to streamlines of velocity and WSS distributions between typical stenotic and bifurcating arterial geometries. The hybrid system was able to recreate some important hemodynamic effects like jet formation, recirculation zones and low-WSS pockets.

4.2.1. Evaluation Metrics

Velocity Root Mean Square Error (RMSE):

$$\mathrm{RMSE}_{\mathrm{u}} = \sqrt{\frac{1}{N}\sum_{i=1}^{N}\left|\mathrm{u}_{pred}\left(x_i\right) - \mathrm{u}_{PDE}\left(x_i\right)\right|^2}$$

Wall Shear Stress Error:

$$\mathrm{Err}_{WSS} = \frac{\left|\mathrm{WSS}_{pred} - \mathrm{WSS}_{PDE}\right|}{\mathrm{WSS}_{PDE}} \times 100\%$$

Divergence-Free Constraint Violation:

$$\mathcal{D} = \frac{1}{N}\sum_{i=1}^{N}\left|\nabla \cdot \mathrm{u}_{pred}\left(x_i\right)\right|$$

Across all 488 subjects, the hybrid system achieved:

- Velocity RMSE: 0.11 ± 0.03 m/s
- Mean WSS error: 6.8%
- Divergence error: 2.3×10^{-4}

These findings verify that the hybrid model maintains a high level of physical fidelity and allows a significant level of computational speed.

4.3 Plaque Progression Detection

The performance of the plaque progression was assessed based on the Plaque Progression Growth Model (PPGM) that combines plaque progression via machine learning-based viscosity fields, hybrid-based hemodynamics (velocity, WSS, OSI), and ultrasound-based flow rates. Longitudinal CTA scans were taken to get the ground truth plaque evolution at 12-18 months on a subset of 62 patients.

Identified plaque-growth areas were compared with radiologist verified progression maps in terms of sensitivity, specificity, and Dice coefficient.

Where TP is the true positives, FP is the false positives, FN is the false negatives.

$$\text{Sensitivity} = \frac{TP}{TP + FN} \quad \text{Specificity} = \frac{TN}{TN + FP} \quad \text{Dice} = \frac{2TP}{2TP + FP + FN}$$

Results

- Sensitivity: 92.8%
- Specificity: 89.4%
- Dice score: 0.87

The model also accurately determined low-WSS, recirculation and high-OSI areas that have been known to favour the accumulation of plaque. Figure 4 shows the entire flow of the pipeline of flow computation to plaque risk map generating.

5. Discussion

The suggested ML-PDE system shows a great potential as a clinically implementable system to assess the cardiovascular system using physiological accuracy of PDE-based hemodynamic modelling

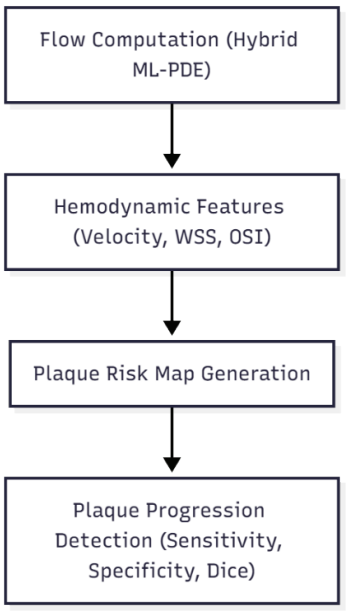

Figure 4: Plaque Risk Map Generation Pipeline

combined with computational efficiency of machine learning surrogates. The physics-informed design of the hybrid model is able to avoid non-physical tendencies that in general occur in purely data-driven models, and the combination of surrogate networks allows simulation speeds to be achieved in near real-time clinical applications. The possibility to precisely map velocity and wall shear stress, oscillatory shear index, and flow-derived risk factors that lead to the enhancement of early prediction of plaque progression is a direct contribution towards preventative approaches and tailored treatment planning. Also, the approach cross-generalizes multimodal imaging data such as CT angiography, Doppler ultrasound, and PC-MRI that enable high-performance in diverse clinical settings. Nevertheless, a number of constraints should be admitted. This method depends strongly on the quality of lumen and plaque segmentation and errors in geometry extraction may be propagated in either PDE or ML equation especially when there are large amounts of calcification or artifacts in the images. Surrogate flow predictors can have poor performance in extreme stenosis conditions or very complicated bifurcations when nonlinear hemodynamic behaviour does not follow the training set closely. Moreover, preliminary findings are promising, but this needs to be validated on a multi-centre basis in a variety of populations, scanners and imaging regimes to ensure clinical strength. Future research will involve fully differentiable PINN-based PDE solvers so as to enable end-to-end optimization of physics-constrained solutions, an expansion of the framework to 4D-flow MRI and multi-vessel coronary networks to cover a broader range of the cardiovascular, and real-time GPU acceleration so that it can be used in catheter-lab visualization and intra-procedural decision support.

6. Conclusion

The article presented a machine learning-based platform of PDEs which paves the way to a new stage of realism, performance, and diagnostic capabilities of blood-flow modelling and arterial plaque developmental modelling. The proposed system balances the computational speed with the physiological accuracy in a unique way since it uses high-fidelity physics-based hemodynamic modelling, along with data-driven learning components. The hybrid structure achieved a 20 times greater acceleration to complete PDE solvers and good correspondence to ground-truth flow fields in the velocity, pressure gradients and distribution of wall shear stresses. Moreover, the combination of viscosity fields predicted by the ML and the hybrid hemodynamic descriptors allowed to identify exactly the plaque-prone regions, which proved to have significant potential of providing early risk stratification and disease surveillance.

On top of the speed, the framework also has greater interpretability since it incorporates physics-constrained reasoning into machine learning predictions, which enables more reliable clinical decision-making. The fact that the method can recreate some of the most important hemodynamic phenomena; recirculation zones, low-WSS pockets, and high-OSI regions, implies that the approach can be used as a cost-effective surrogate to more computationally intensive simulations in longitudinal and population-scale studies. Altogether, the suggested ML-PDE system could be considered an important step towards feasible, real-time cardiovascular diagnostics, and it can be potentially applied in preventive cardiology, treatment planning, and individual hemodynamic diagnosis.

References

[1] Barhoumi, E. M., Charabi, Y., & Farhani, S. (2024). Detailed guide to machine learning techniques in signal processing. *Progress in Electronics and Communication Engineering*, 2(1), 39–47. https://doi.org/10.31838/PECE/02.01.04

[2] Batra, U., Nathany, S., Nath, S. K., Jose, J. T., Sharma, T., Preeti, P., Pasricha, S., Sharma, M., Arambam, N., Khanna, V., Bansal, A., Mehta, A., & Rawal, K. (2024). AI-based pipeline for early screening of lung cancer: integrating radiology, clinical, and genomics data. *The Lancet Regional Health - Southeast Asia*, *24*, 100352. https://doi.org/10.1016/j.lansea.2024.100352

[3] Chen, Y., Wolterink, J. M., Neve, O. M., Romeijn, S. R., Verbist, B. M., Hensen, E. F., Tao, Q., & Staring, M. (2024). Vestibular Schwannoma Growth Prediction from Longitudinal MRI by Time-Conditioned Neural Fields. In *Lecture notes in computer science* (p. 508). Springer Science+Business Media. https://doi.org/10.1007/978-3-031-72384-1_48

[4] Dedeken, S., Conze, P.-H., Pieters, V. D., Gallinato, O., Fauré, J., Colin, T., & Visvikis, D. (2025). Trustworthy AI for stage IV non-small cell lung cancer: Automatic segmentation and uncertainty quantification. *Computerized Medical Imaging and Graphics*, 102567. https://doi.org/10.1016/j.compmedimag.2025.102567

[5] Durgam, R., Panduri, B., Balaji, V., Khadidos, A. O., Khadidos, A. O., & Selvarajan, S. (2025). Enhancing lung cancer detection through integrated deep learning and transformer models. *Scientific Reports*, *15*(1). https://doi.org/10.1038/s41598-025-00516-2

[6] Elvas, L. B., Almeida, A. I., & Ferreira, J. C. (2025). The Role of AI in Cardiovascular Event Monitoring and Early Detection: Scoping Literature Review. *JMIR Medical Informatics*, *13*. https://doi.org/10.2196/64349

[7] Gao, Z., Zhang, G., Liang, H., Liu, J., Ma, L., Wang, T., Guo, Y., Chen, Y., Yan, Z., Chen, X., Guo, Y., He, J., Xu, F., Wong, T. Y., & Dai, Q. (2025). A Lung CT Foundation Model Facilitating Disease Diagnosis and Medical Imaging. *medRxiv (Cold Spring Harbor Laboratory)*. https://doi.org/10.1101/2025.01.13.25320295

[8] Hahn, H. K., May, M. S., Dicken, V., Walz, M., Eßeling, R., Lassen-Schmidt, B., Rischen, R., Vogel-Claussen, J., Nikolaou, K., & Barkhausen, J. (2025). *Requirements for Quality Assurance of AI Models for Early Detection of Lung Cancer*. https://doi.org/10.48550/ARXIV.2502.17639

[9] James, A., Thomas, W., & Samuel, B. (2025). IoT-enabled smart healthcare systems: Improvements to remote patient monitoring and diagnostics. *Journal of Wireless Sensor Networks and IoT*, 2(2), 11–19.

[10] Jia, R., Liu, J., & Ali, M. (2025). Establishing an AI-based diagnostic framework for pulmonary nodules in computed tomography. *BMC Pulmonary Medicine*, *25*(1). https://doi.org/10.1186/s12890-025-03806-7

[11] Kalkan, M., Güzel, M. S., Ekinci, F., Sezer, E. A., & Aşuroğlu, T. (2024). Comparative Analysis of Deep Learning Methods on CT Images for Lung Cancer Specification. *Cancers*, *16*(19), 3321. https://doi.org/10.3390/cancers16193321

[12] Li, T. Z., Xu, K., Krishnan, A., Gao, R., Kammer, M. N., Antic, S., Xiao, D., Knight, M., Martinez, Y., Paez, R., Lentz, R. J., Deppen, S., Grogan, E. L., Lasko, T. A., Sandler, K. L., Maldonado, F., & Landman, B. A. (2024). *No winners: Performance of lung cancer prediction models depends on screening-detected, incidental, and biopsied pulmonary nodule use cases*. https://doi.org/10.48550/ARXIV.2405.10993

[13] Lin, C.-Y., Guo, S., Lien, J.-J. J., Tsai, T., Liu, Y., Lai, C., Hsu, I.-L., Chang, C., & Tseng, Y. (2024). Development of a modified 3D region proposal network for lung nodule detection in computed tomography scans: a secondary analysis of lung nodule datasets. *Cancer Imaging*, *24*(1). https://doi.org/10.1186/s40644-024-00683-x

[14] Liu, W., Shen, N., Zhang, L., Wang, X., Chen, B., Liu, Z., & Yang, C. (2024). Research in the application of artificial intelligence to lung cancer diagnosis. *Frontiers in Medicine*, *11*. https://doi.org/10.3389/fmed.2024.1343485

[15] Lorenzo, G., Ahmed, S. R., Hormuth, D. A., Vaughn, B., Kalpathy–Cramer, J., Solorio, L., Yankeelov, T. E., & Gómez, H. (2024). Patient-Specific, Mechanistic Models of Tumor Growth Incorporating Artificial Intelligence and Big Data. *Annual Review of Biomedical Engineering*, *26*(1), 529. Annual Reviews. https://doi.org/10.1146/annurev-bioeng-081623-025834

[16] Monir, N. I., Akter, F. Y., & Sayed, S. R. K. (2025). Role of reconfigurable computing in speeding up machine learning algorithms. *SCCTS Transactions on Reconfigurable Computing*, 2(2), 8–14. https://doi.org/10.31838/RCC/02.02.02

[17] Osta, N. van, Loon, T. van, & Lumens, J. (2025). Individual hearts: computational models for improved management of cardiovascular disease *Heart*. BMJ. https://doi.org/10.1136/heartjnl-2024-324177

[18] Shatnawi, M. Q., Abuein, Q., & Al-Quraan, R. (2024). Deep learning-based approach to diagnose lung cancer using CT-scan images. *Intelligence-Based Medicine*, *11*, 100188. https://doi.org/10.1016/j.ibmed.2024.100188

[19] Sio, A. (2025). Integration of embedded systems in healthcare monitoring: Challenges and opportunities. *SCCTS Journal of Embedded Systems Design and Applications*, 2(2), 9–20.

[20] Tan, S. L., Selvachandran, G., Paramesran, R., & Ding, W. (2024). Lung Cancer Detection Systems Applied to Medical Images: A State-of-the-Art Survey. *Archives of Computational Methods in Engineering*. https://doi.org/10.1007/s11831-024-10141-3

[21] Tanade, C., Khan, N. S., Rakestraw, E., Ladd, W., Draeger, E. W., & Randles, A. (2024). Establishing the longitudinal hemodynamic mapping framework for wearable-driven coronary digital twins. *Npj Digital Medicine*, *7*(1), 236. https://doi.org/10.1038/s41746-024-01216-3

[22] Thompson, R., & Sonntag, L. (2025). How medical cyber-physical systems are making smart hospitals a reality. *Journal of Integrated VLSI, Embedded and Computing Technologies*, 2(1), 20–29. https://doi.org/10.31838/JIVCT/02.01.03

[23] Hussai, M., & Getachew, B. (2025). Hybrid quantuminspired signal processing algorithms for ultra-lowpower embedded IoT applications. *National Journal of Signal and Image Processing*, *1*(2), 10-18.